
ARTICLE

Lattice expansion in ZrN and Dy_{0.3}Zr_{0.7}N irradiated by 200 MeV Xe ions

Seiya Takaki*, Masahide Takano and Norito Ishikawa

Japan Atomic Energy Agency, 2-4 Shirakata, Tokai-mura, Naka-gun, Ibaraki-ken, 319-1195, Japan

Lattice parameter and heterogeneous strain in ZrN and Dy_{0.3}Zr_{0.7}N irradiated with 200 MeV Xe ions were examined by conventional X-ray diffraction (XRD) analysis to obtain fundamental knowledge on the microstructure evolution induced by fission fragments in nitride fuels, which is important for the development of inert matrix fuels for transmutation of minor actinides (MA). The XRD measurements revealed that no phase transformation induced by irradiation occurred and indicated an increase in the unit cell parameter and the accumulation of heterogeneous microstrain with increasing ion fluence. These data were fitted with a single-impact model of damage accumulation. It is indicated that cylindrical defects which induce increasing lattice expansion and lattice distortion are formed in ZrN and Dy_{0.3}Zr_{0.7}N.

Keywords: nitride fuels; ZrN; MA transmutation; radiation damage; high density electronic excitation; ion track; X-ray diffraction

1. Introduction

Zirconium nitride (ZrN) is one of the candidate inert matrix of the nitride fuel for transmutation of minor actinides (MAs: Np, Am, Cm) in a subcritical core with an accelerator driven system (ADS) [1,2]. For this system, transuranium (TRU) nitrides consisting of Pu and MAs are diluted with 55~70 mol% ZrN, which enables to control local peaking of such fuels. The fuel is single-phase solid solution between ZrN and TRU nitrides, so called MA-bearing nitride fuel.

Among the radiation sources under the environments of MA nitride fuels, radiation damage induced by fission fragments (FFs) with kinetic energies ranging from 70 to 100 MeV, is one of the crucial issues. FFs induce high density electronic excitation along the penetrating path to result in the formation of cylindrical or tubular defects, so called ion tracks. In the ion tracks, amorphous region or voids surrounded by a defective region forms in variety of oxide ceramics [3]. On the other hand, very little information on such damage in ZrN and nitride fuels are available.

For investigating feasibility, fabrication and properties of MA-bearing nitride fuels, lanthanide nitrides have been utilized as a surrogate materials of TRU nitrides, because of the identical crystal structure and similar material properties [4,5]. Especially, DyN, which has lattice parameter very close to that of PuN and vaporization behavior similar to that of AmN, forms a complete solid solution with ZrN [6].

The present study aims to gain insights into high density electronic excitation in ZrN and Dy_{0.3}Zr_{0.7}N as a

surrogate materials of MA-bearing nitride fuels, irradiated with swift heavy ions as a function of 200 MeV Xe ion fluence. The irradiated materials were analyzed by conventional X-ray diffraction (XRD) measurements to evaluate the microstructure evolution.

2. Experimental**2.1. Sample preparation**

DyN and ZrN were prepared from corresponding metals through an intermediate synthesis of the hydrides. The metal rods were heated at 693 K in a purified Ar-20%H₂ mixed gas flow for 20 h for hydrogenation. The hydrides were pulverized into coarse powders, respectively. These powders were heated at 1073 K for 1 h and subsequently at 1573 K for 4 h in a purified N₂ gas flow for nitridation, respectively.

The powders of DyN and ZrN were mixed at 30/70 molar ratio. The mixtures were ground by a high-speed planetary ball mill with a tungsten carbide (WC) pot and balls in order to ensure the homogeneous and fine powder mixtures. The mixtures were molded at a pressure of 200 MPa and then loaded into an electric furnace. The heat treatment for solid solution formation was performed at 1873 K for 6 h in the N₂ gas flow.

The sintered pellets of ZrN and Dy_{0.3}Zr_{0.7}N solid solution were obtained by the similar way to the solid solution preparation at 1973 K for 6h in the N₂ gas flow. The sintered pellets were evaluated to be about 90% of theoretical density, which was calculated from the dimensions and the mass. The impurity oxygen content was 0.2 wt% and the average grain size was 5 μm.

*Corresponding author. Email: takaki.seiya@jaea.go.jp

2.2. Swift heavy ions irradiation

Surface of the 2 mm thick specimens were polished and then irradiated with 200 MeV Xe ions at ambient temperature under vacuum. The irradiation was performed by using a tandem ion accelerator at Japan Atomic Energy Agency, with the fluence between $1 \times 10^{11} \text{ cm}^{-2}$ and $1 \times 10^{14} \text{ cm}^{-2}$. The electronic (S_e) and nuclear (S_n) stopping power of 200 MeV Xe ions were calculated to be about 31 keV nm^{-1} and below 0.05 keV nm^{-1} at the surface region, respectively, by using the SRIM2012 (Stopping and Range of Ions in Matter) code [7] with a threshold displacement energy (E_d) of 40 eV for cation and 20 eV for anion, and using theoretical density derived from lattice parameter of ZrN and $\text{Dy}_{0.3}\text{Zr}_{0.7}\text{N}$. The values of E_d are based on the estimation of ZrC [8]. **Figure 1** shows that S_e becomes dominant compared to the one induced by FFs in nuclear fuel/target materials (around 20 keV nm^{-1}). The higher electronic stopping power (31 keV nm^{-1}) is used in the present study to investigate the high density electronic excitation damage in Zr-based nitride, to make it easier to detect microstructural change by depositing more energy to the materials.

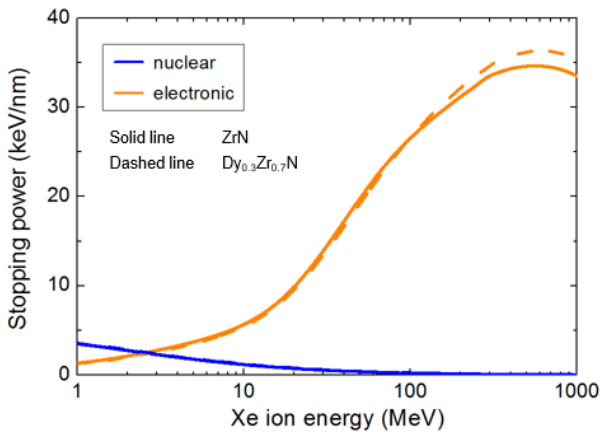


Figure 1. Ion energy dependence of electronic stopping power (S_e) and nuclear stopping power (S_n) for Xe ions. Target materials are ZrN and $\text{Dy}_{0.3}\text{Zr}_{0.7}\text{N}$.

2.3. X-ray diffraction analysis

In order to investigate the change in the lattice structure of irradiated ZrN and $\text{Dy}_{0.3}\text{Zr}_{0.7}\text{N}$, we used a conventional Cu-K α X-ray diffractometer. XRD patterns were recorded at room temperature in a 2θ range from 20° to 150° with 0.04° steps; the acquisition time was 5 s per step.

3. Results and discussion

Figure 2 shows XRD patterns recorded on the surface of ZrN irradiated with 200 MeV Xe ions and non-irradiated samples. The peaks of non-irradiated samples correspond to the NaCl-type structure. In **Figure 2** (a), additional peaks can't be observed at any fluence

compared to non-irradiated patterns in all the measured range, revealing that no phase transformation induced by irradiation occurred. In **Figure 2** (b), broadening of the diffraction peaks and shift towards lower angles are confirmed with increasing ion fluence. Such tendencies were also observed on the $\text{Dy}_{0.3}\text{Zr}_{0.7}\text{N}$ samples. The peak shift indicates an increase in the lattice parameter for both nitrides. The peak broadening is attributed to the irradiation-induced structural distortion and the change in crystallite size, respectively. In order to determine the source of the peak broadening, we utilized Williamson-Hall plots [9], as shown in **Figure 3**. The plots were constructed from the XRD data on $\text{Dy}_{0.3}\text{Zr}_{0.7}\text{N}$ irradiated at each fluence, where λ is the wave length of Cu-K α , β is the induced peak broadening, the slope depends on the heterogeneous strain, and y -intercept is inversely proportional to the grain size of irradiated $\text{Dy}_{0.3}\text{Zr}_{0.7}\text{N}$. This analysis indicated that the peak broadening in the irradiated $\text{Dy}_{0.3}\text{Zr}_{0.7}\text{N}$ is due to increasing heterogeneous strain and crystallite size.

Figure 4 (a) shows the heterogeneous strain values (ε) as a function of the ion fluence for ZrN and $\text{Dy}_{0.3}\text{Zr}_{0.7}\text{N}$, while **Figure 4** (b) shows the lattice parameter evolution ($\Delta a/a_0$) with the irradiation fluence, which has been derived from the peak shift of the XRD profiles for ZrN and $\text{Dy}_{0.3}\text{Zr}_{0.7}\text{N}$. Both data show monotonic increase followed by saturation. This behavior is discussed by using a single-impact mechanism for damage accumulation [10]. In this model, an ion to penetrate a certain volume of the material fully modifies the region, assuming cylindrical shape and subsequent overlaps of the region give no modification to the materials. The single impact model is given as;

$$A = A_{\text{sat}}[1 - \exp(-\Phi\pi(D/2)^2)] \quad (1)$$

where A is the parameter being modified, A_{sat} is the saturation value of the parameter, Φ is the irradiation fluence, and D is the effective diameter, in which the modification of interest is induced. The solid and dashed curves shown in **Figure 4** represent the fitted results of data obtained by irradiated ZrN and $\text{Dy}_{0.3}\text{Zr}_{0.7}\text{N}$, respectively. This fitting procedure gives a maximum strain value of $0.28 \pm 0.01\%$ and a saturation lattice parameter of $0.15 \pm 0.01\%$ for $\text{Dy}_{0.3}\text{Zr}_{0.7}\text{N}$. The A_{sat} of unit cell is a half of or less than those obtained by Takano [11] for alpha-particle irradiations in the TRU nitrides, suggesting that damage production by swift heavy ions in lanthanide and TRU nitrides is less efficient than that of alpha particle self-irradiation.

The D values of $\Delta a/a_0$ and ε corresponding to D_a and D_ε are given in **Table 1**. D_a of ZrN is smaller than that of $\text{Dy}_{0.3}\text{Zr}_{0.7}\text{N}$. In this analysis, we assume that $\Delta a/a_0$ of ZrN reach saturation similar with $\text{Dy}_{0.3}\text{Zr}_{0.7}\text{N}$. Although the curve of ZrN in **Figure 4** (b) does not reach saturation, the dependence of $\Delta a/a_0$ on fluence is smaller than that of $\text{Dy}_{0.3}\text{Zr}_{0.7}\text{N}$, which supports the size relation of D_a between ZrN and $\text{Dy}_{0.3}\text{Zr}_{0.7}\text{N}$. In this study, the S_e values are almost same between ZrN and $\text{Dy}_{0.3}\text{Zr}_{0.7}\text{N}$.

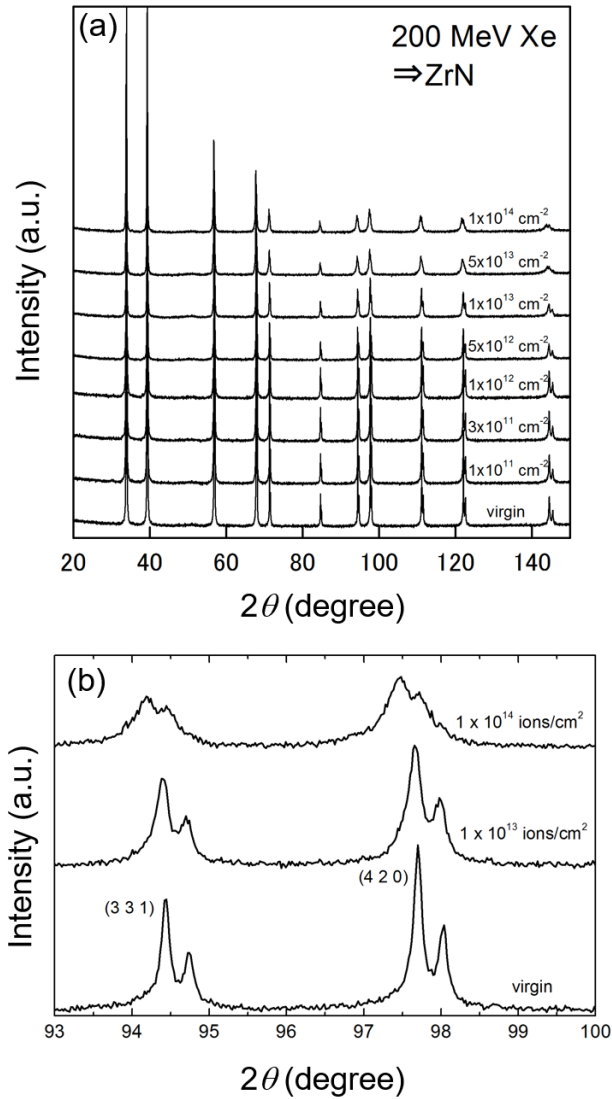


Figure 2. (a) XRD patterns of irradiated and non-irradiated ZrN. (b) Representative XRD patterns in Figure 2 (a) are shown in a range from 93° to 100° (2θ).

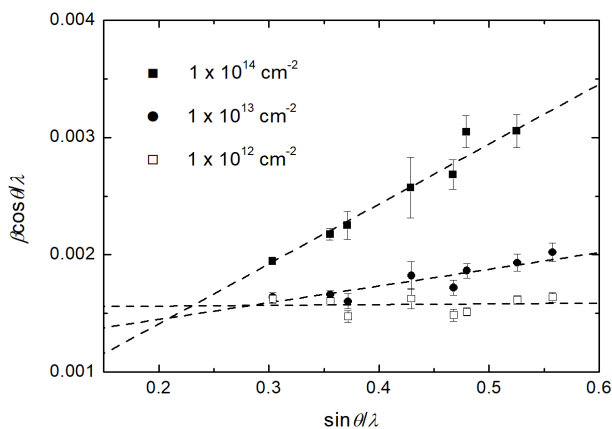


Figure 3. Williamson-Hall plots of representative XRD data corrected from irradiated $\text{Dy}_{0.3}\text{Zr}_{0.7}\text{N}$.

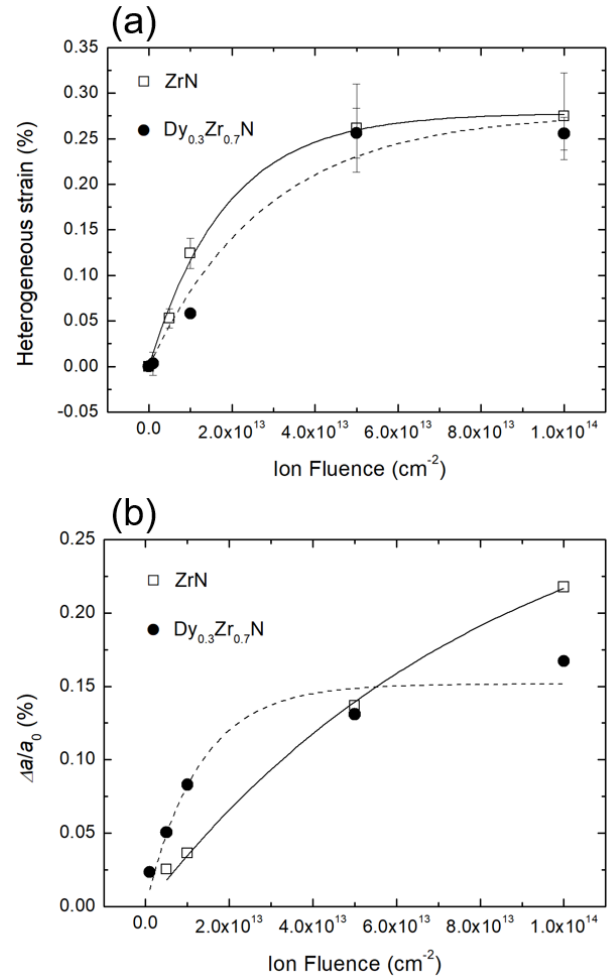


Figure 4. Ion fluence dependences of (a) heterogeneous strain and (b) lattice parameter change for ZrN and $\text{Dy}_{0.3}\text{Zr}_{0.7}\text{N}$ irradiated with 200 MeV Xe ions.

Table 1. Effective diameters extracted from the fits to XRD experimental data with Eq. (1).

	D_a (nm)	D_e (nm)
ZrN	1.23 ± 0.12	2.63 ± 0.13
$\text{Dy}_{0.3}\text{Zr}_{0.7}\text{N}$	3.17 ± 0.41	2.12 ± 0.35

It is considered that the different size of D_a is attributed to the difference of characteristic properties between ZrN and $\text{Dy}_{0.3}\text{Zr}_{0.7}\text{N}$. For example, thermal conductivity of (TRU,Zr)N solid solutions decrease with increasing TRU fraction [12]. In addition, the thermal conduction in Zr-based lanthanides and TRU nitride solid solutions is principally derived from electronic conduction, so it is suggested that the difference of thermal properties has an influence on the deposition of energy through the electronic system of target under irradiation. Finally, it is considered that the ion tracks that induce the lattice expansion are easier to form in (Dy,Zr)N than in ZrN, so D_a of ZrN is smaller than that of $\text{Dy}_{0.3}\text{Zr}_{0.7}\text{N}$. In case of ZrN, the difference between D_a and D_e indicates a

core-shell track morphology. The core is fully modified, such that a larger unit cell parameter exhibited, while the shell is defect rich, such that heterogeneous strain occurs there. On the other hand, D_a of $Dy_{0.3}Zr_{0.7}N$ is larger than D_e , which suggest that the increase in unit cell parameter is attributable to not only modification but also the change in composition of (Dy,Zr)N.

4. Summary

The change in lattice parameter and the structure of defects induced by high-density electronic excitation in ZrN and $Dy_{0.3}Zr_{0.7}N$ have been investigated by the irradiation with 200 MeV Xe ions and by means of XRD analysis. Followings are drawn as summaries from the present study.

XRD patterns showed that the NaCl-type crystal structures are retained with fluence up to $1 \times 10^{14} \text{ cm}^{-2}$, although the peak broadening and shift corresponding to the increase in heterogeneous strain and lattice expansion were observed. The fitting analysis of ion fluence dependence of lattice expansion indicated that the sizes of region that induces the lattice expansion are different between ZrN and $Dy_{0.3}Zr_{0.7}N$, and the difference is considered to be attributed to the different thermal properties.

Further study on the structural and accumulation behavior of ion tracks in Zr-based nitride is expected to contribute to gain insight into the fundamentals of defect formation and accumulation in the MA-bearing nitride fuel.

Acknowledgements

The authors are deeply grateful to technical staffs at Tandem ion accelerator facility in Japan Atomic Energy Agency-Tokai during swift heavy ion irradiation. The author is thankful to Messrs. T. Tobita, A. Ito and H. Kato for their support in experiments.

References

- [1] H. Oigawa, K. Tsujimoto, K. Nishiha, T. Sugawara, Y. Kurata, H. Takei, S. Saito, T. Sasa and H. Obayashi, Role of ADS in the back-end of the fuel cycle strategies and associated design activities: The case of Japan, *J. Nucl. Mater.* 415 (2011), pp. 229-236.
- [2] J. Wallenius, S. Pillon and L. Zaboudko, Fuels for accelerator-driven systems, *Nucl. Instrum. Methods Phys. Res., Sect. A* 562 (2006), pp. 625-629.
- [3] M. Toulemonde, W. Assmann, C. Dufour, A. Meftah, F. Studer and C. Trautmann, Experimental phenomena and thermal spike model description of ion tracks in amorphisable inorganic insulators, *Matematisk-fysiske Meddelelser* 52 (2006), pp. 263-292.
- [4] M. Takano, A. Itoh, M. Akabori and K. Minato, Hydrolysis reactions of rare-earth and americium mononitrides, *J. Phys. Chem. Solids*, 66(24) (2005), pp. 697-700.
- [5] M. Takano, Experimental evaluation of solid solubility of lanthanide and transuranium nitrides into ZrN matrix, *J. Nucl. Mater.* 440 (2013), pp. 489-494.
- [6] M. Takano, S. Tagami, K. Minato, T. Kozaki and S. Sato, Lattice thermal expansion of (Dy,Zr)N solid solutions, *J. Alloys Compd.* 439 (2007), pp. 215-220.
- [7] J.F. Ziegler, J.P. Biersack and U. Littmark, *The Stopping and Range in ions in Solids*. Pergamon, New York (1985).
- [8] D. Gosset, M. Dollé, D. Simeone, G. Baldinozzi and L. Thomé, *J. Nucl. Mater.* 373 (2008), pp. 123-129.
- [9] C.J. Howard and T.M. Sabine, X-ray diffraction profiles from neutron-irradiated magnesium oxide, *J. Phys. C Solid State*, 7 (1974), pp. 3453-3466.
- [10] J. Jagielski and L. Thome, Damage accumulation in ion-irradiated ceramics, *Vacuum*, 81 (2007), pp. 1352-1356.
- [11] M. Takano, H. Hayashi and K. Minato, Thermal expansion and self-irradiation damage in curium nitride lattice, *J. Nucl. Mater.* 448 (2014), pp. 66-71.
- [12] T. Nishi, M. Takano, K. Ichise, M. Akabori and Y. Arai, Thermal conductivities of Zr-based transuranium nitride solid solutions, *J. Nucl. Sci. Technol.* 48 (2011), pp. 359-365.